

AN3008: Metacomplex Formation & Binding Affinity of Multivalent Binding Partners

Sophia Kenrick, Ph.D. and Dan Some, Ph.D., Wyatt Technology

Summary

Multivalent binding plays a crucial role in protein-protein interactions, including cell signaling pathways, immunological responses, and self-assembly of structural elements. However, standard analytical techniques for measuring macromolecule interactions require one binding partner to be immobilized on a surface, leading to errors when both binding partners are multivalent. [Composition-gradient multi-angle light scattering \(CG-MALS\)](#) is unique in its ability to quantify such interactions to yield affinity and stoichiometry of complexes forming in solution. We investigate metacomplex formation in the hetero-association of a multivalent antigen—streptavidin (SA)—and a bivalent antibody (Ab) using CG-MALS.

Automated composition gradients were created using a [Calypso®](#) connected to an inline UV/Vis concentration detector and [DAWN® MALS instrument](#). Single-component concentration gradients were used to quantify any self-association, and a dual-component “crossover” composition gradient assessed hetero-association (Figure 1). The data indicated that SA and Ab associate into complexes with higher molecular weight than a simple 1:1 or 2:1 stoichiometry (Figure 2). Since neither protein was found to self-associate, the higher-order stoichiometries must have resulted from the multivalent nature of the two binding partners.

The [CALYPSO™ software](#) enabled evaluation of three hetero-associating models: ‘ISA’, the infinite self-association of (SA)(Ab) base units into n:n complexes; ISA with additional 1:2 and 2:1 terms; and ‘2x2’, a model that allows for all possible complexes between two bivalent proteins with equivalent binding sites. Despite having the fewest degrees of freedom, the 2x2 model provides the best fit, yielding affinities of 34 nM per binding site.

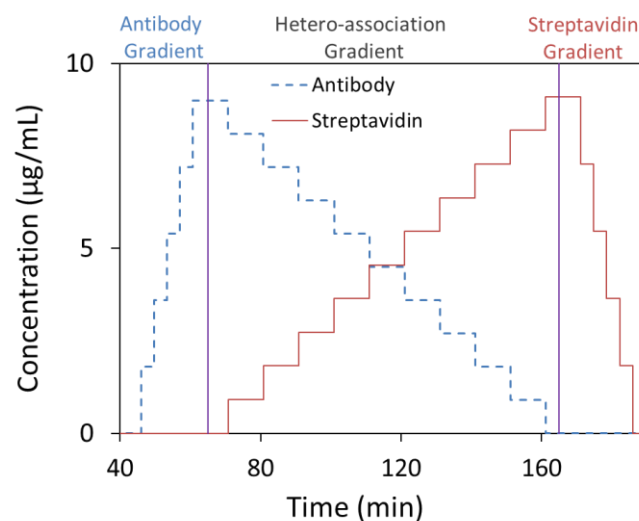


Figure 1: Composition-gradient method for quantifying the interaction between streptavidin and an anti-streptavidin antibody.

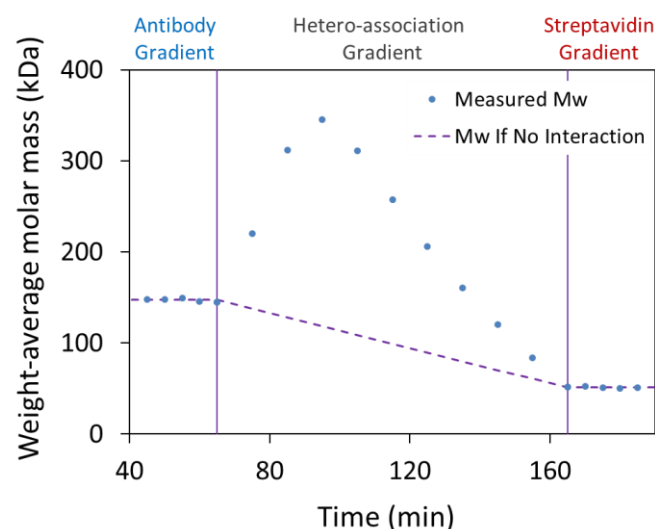


Figure 2: Weight-average molar mass (M_w) at equilibrium for each composition shown in the top figure. During the hetero-association gradient, formation of SA-Ab complexes results in an increase in M_w .

Introduction

Standard analytical techniques for probing macro-molecular interactions, such as SPR and ELISA, require one binding partner to be immobilized on a surface in order to quantify the binding affinity. For simple 1:1 association and for some 1: n interactions, this physical tethering usually does not significantly impact the equilibrium dissociation constants (K_d) that are measured. When both binding partners are multivalent, however, immobilizing one ligand can lead to erroneous estimates of the binding affinity by orders of magnitude due to avidity effects at the surface, mass transport limitations, and incorrect assumptions about the stoichiometry of the interaction. In contrast, composition-gradient multi-angle light scattering (CG-MALS) measures interactions entirely in solution, allowing all possible binding stoichiometries to occur and providing simultaneous quantification of self- and hetero-interactions, metacomplex formation, and

other multivalent interaction.¹ Here, we use CG-MALS to investigate the complex stoichiometries that result from the binding of an anti-streptavidin antibody (Ab) to the homo-tetramer streptavidin (SA) (Figure 3).

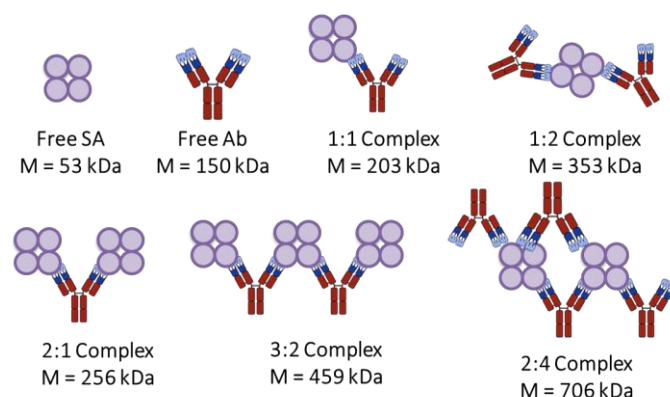


Figure 3: Some of the possible complexes formed between SA and Ab. The two identical binding sites of Ab can bind one or two SA molecules. SA's homo-tetrameric structure provides four possible binding sites and enables additional self-assembly of complexes in solution.

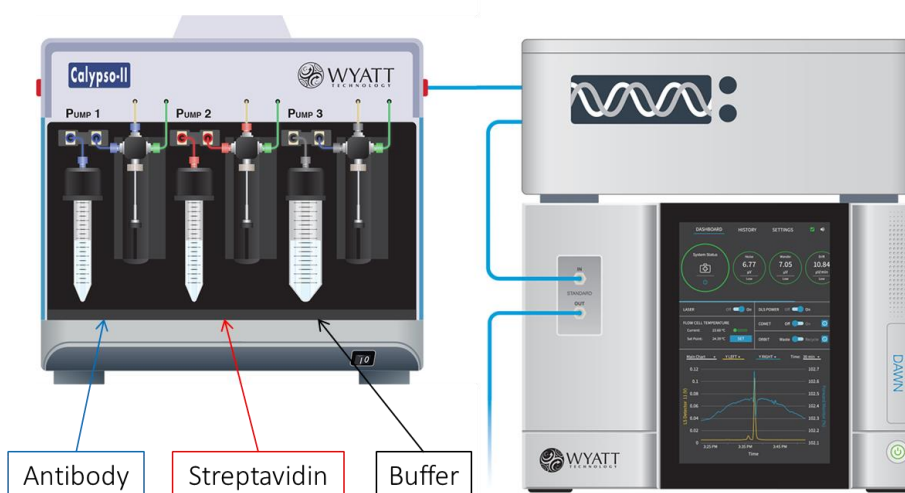


Figure 4: Calypso system hardware setup with inline UV/Vis concentration detector and DAWN MALS detector

Materials and Methods

Reagents and instrumentation

CG-MALS experiments were performed with a Calypso composition-gradient system that prepared and delivered different compositions of protein and buffer to an inline UV/Vis detector and DAWN MALS instrument (Figure 4).

The anti-streptavidin antibody was kindly provided by Dr. Shawn Cao of Amgen. Streptavidin and antibody were

diluted to a stock concentration of 10 $\mu\text{g}/\text{mL}$ in a phosphate buffered saline (50 mM NaCl) for a total of $\sim 100 \mu\text{g}$ each protein per experiment. Solutions were filtered to 0.02 μm and loaded on the Calypso.

Determination of equilibrium association constant and stoichiometry

Experiment control, data acquisition and analysis, including all data modelling, were performed with CALYPSO™ software. A fully automated Calypso method was run, consisting of single-component concentration gradients

to quantify any self-association and a dual-component “crossover” composition gradient to assess the hetero-association behavior (Figure 1). For each composition, 0.8 mL of protein solution at the appropriate composition was injected into the UV/Vis and MALS detectors. The flow was then stopped to allow the solution to come to equilibrium within the MALS flow cell. For single protein gradients the flow was stopped for 120 s. The stop-flow time was increased to 500 s for the crossover gradient.

Results and Discussion

MALS signals are proportional to the product of weight-average molar mass, M_w , and concentration. Figure 5 presents the measured light scattering overlaid with the signal expected for a standard antibody-antigen 1:2 interaction. The increased light scattering signal in the hetero-association gradient region indicates that Ab and SA associate into complexes with a higher molecular weight than a simple 1:1 or 1:2 stoichiometric ratio. Since neither protein was found to self-associate under these conditions, the higher-order stoichiometries must have resulted from the multivalent nature of the two binding partners.

In a “crossover” hetero-association gradient, the composition with the maximum light scattering signal occurs at the overall stoichiometric ratio of the interaction. This ratio, combined with the magnitude of M_w , yields the absolute stoichiometry of the interaction. Figure 6 compares the measured M_w to simulations of three simple SA:Ab stoichiometries. For each simulation, the affinity per binding site was considered constant, $K_d = 0.2$ nM. Although the measured data reach a maximum near the 1:1 molar ratio, the maximum measured M_w (~350 kDa) is significantly larger than the maximum molecular weight for the 1:1 model (~200 kDa, dotted red line). A model considering two Ab bound per SA molecule approaches the correct maximum M_w (~330 kDa, solid purple line). However, this maximum occurs at the wrong composition compared to the measured data, and this simulated model significantly underestimates the measured M_w for all compositions with excess SA.

Clearly the data indicate the presence of higher-order complexes with an overall stoichiometric ratio of 1:1, i.e., $(SA)_2(Ab)_2$, $(SA)_3(Ab)_3$, etc. This result seems surprising as SA’s four possible binding sites compared to the two on Ab suggest that complexes can occur with higher SA:Ab ratios, such as 4:2 shown in Figure 1. The complex that

saturates the most binding sites would have an overall stoichiometric ratio of 2(SA):1(Ab). However, the crystal structure of streptavidin shows a dimer of dimers with two-fold symmetry, rather than a tetramer with four-fold symmetry² which could explain this propensity to form 1:1 metacomplexes rather than 2:1 metacomplexes. Interestingly, a similar 2:1 stoichiometric ratio for macromolecular interactions has also been observed with DNA aptamers raised against streptavidin.³⁻⁵

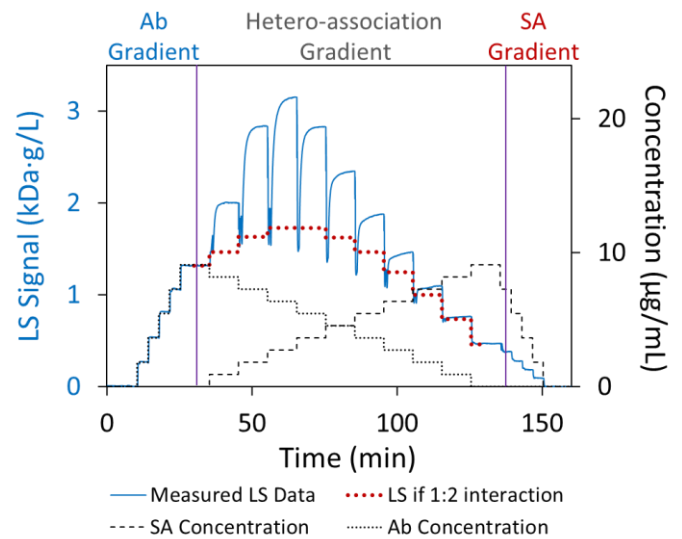


Figure 5: Light scattering and concentration data for the interaction between SA and Ab. The association is greater than can be explained by 1:2 interaction (bold-dotted red line).

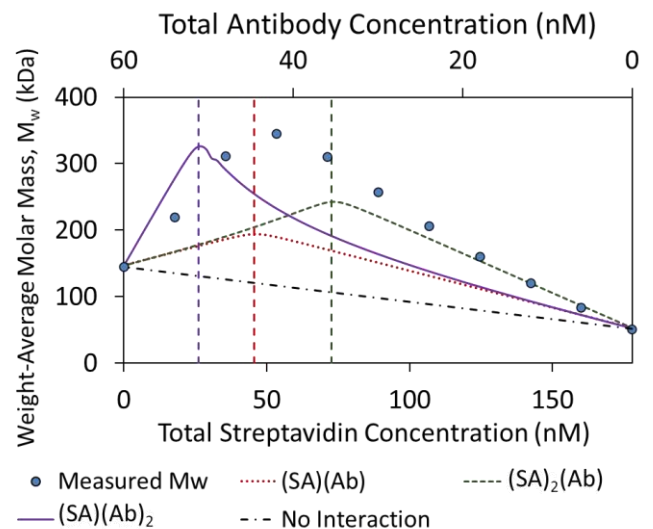


Figure 6: Measured M_w values (see Figure 2) compared to simulated M_w for 1:1, 1:2 and 2:1 stoichiometries with $K_d = 0.2$ nM. The position of the peak in the measured M_w indicates that the largest complexes form with stoichiometry $n:n$ (dotted red line) compared to $2n:n$ (dashed green line) or $n:2n$ (solid purple line).

To characterize the SA-Ab interaction, three different models are considered: (1) 'ISA' - infinite self-association of (SA)(Ab) base units into $[(SA)(Ab)]_n$ (i.e., $n:n$) complexes; (2) ISA with additional 1:2 and 2:1 terms; and (3) '2x2' - an analysis that assumes all possible complexes formed between two dimers, each of which possesses two equivalent binding sites for the other.

1. First pass analysis: Infinite self-association of 1:1 stoichiometries $[(SA)(Ab)]_n$

In the infinite self-association (ISA) model, SA and Ab bind with some affinity to form a 1:1 base unit $[(SA)(Ab)]$. This base unit then self-associates indefinitely, with each base unit adding to the growing chain with constant affinity. Modelling the data by this association scheme, Ab binds SA with best-fit affinity $K_{d,1:1} = 5$ nM, and the $[(SA)(Ab)]$ base units self-assemble with a best fit of $K_{d,ISA} = 44$ nM.

Results of the fit are plotted in Figure 7. While this model clearly accounts for the majority of the interaction with a quite good fit, it is unsatisfying in two respects. First, the results imply that the formation of the core base unit occurs with 10-fold stronger affinity than the interaction between base units, even though the same binding sites are involved. Since the ISA model does not include cooperativity, it is possible that steric hindrance or some other cooperative effect causes the affinity to decrease, and the fit provides an average K_d value for 2:2, 3:3 and higher complexes. Second, the assumption of at least two binding sites on each protein suggests that other stoichiometries should be present, e.g. 1:2, 2:1, 2:3, 3:2, etc. These complexes are not taken into account.

2. Refined analysis: ISA + 1:2 and 2:1 complexes

The analysis may be refined by adding to the model the first two complexes that are not of 1:1 ratio, namely $(SA)(Ab)_2$ and $(SA)_2(Ab)$. Their equilibrium constants were not constrained in the model in any way to match those of the 1:1 or ISA interactions. Fitting the refined model to the data provides an improved fit: χ^2 decreased from 0.485 to 0.26. Perhaps more significantly, with this addition the K_d values for the base complex ($K_{d,1:1}$), ISA ($K_{d,ISA}$) and the 1:2 and 2:1 complexes ($K_{d,1:2}$ and $K_{d,2:1}$) converge to a tight range, 23 ± 7 nM. The results are shown in Figure 8. This convergence is more in line with expectations for equivalent binding sites, though the expected terms are still missing for 2:3, 3:2 and other complexes.

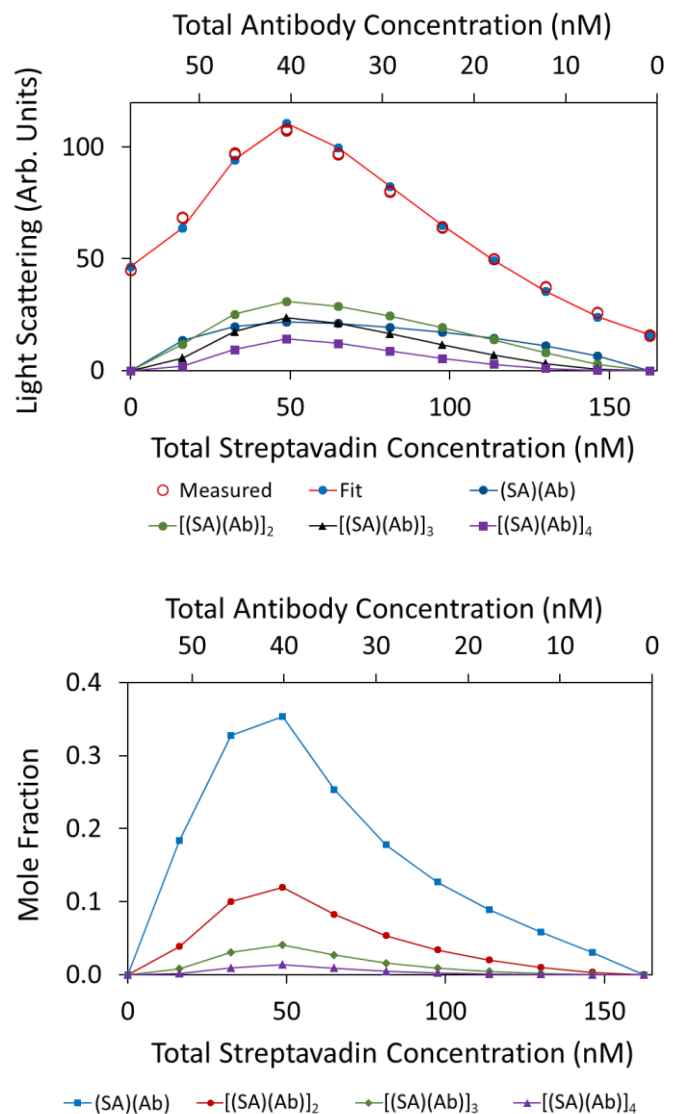


Figure 7: ISA model. Top: The best fit (blue circles) for the measured light scattering data (red open circles). Contributions from (SA)(Ab) and ISA species: $[(SA)(Ab)]_2$, $[(SA)(Ab)]_3$, etc. are shown up to 4th order; roughly up to 6th order are significant. Bottom: For each composition, the molar distribution of species in solution. In both graphs, SA and Ab monomer contributions are left off for clarity.

2. Final analysis: 2x2 model

The success of the refined model, producing similar single binding site K_d values for each term, suggests that a model accounting for all possible complexes formed by two molecules, each of which has two equivalent binding sites for the other, with no cooperativity, would be the best representation of the SA-Ab interaction. Such a model, denoted '2x2', is included in the CALYPSO software: it assumes all possible $n:n$, $n:n-1$ and $n-1:n$ complexes, up to any selected $n > 2$, with a single equilibrium constant K_d representing all single-site interactions.

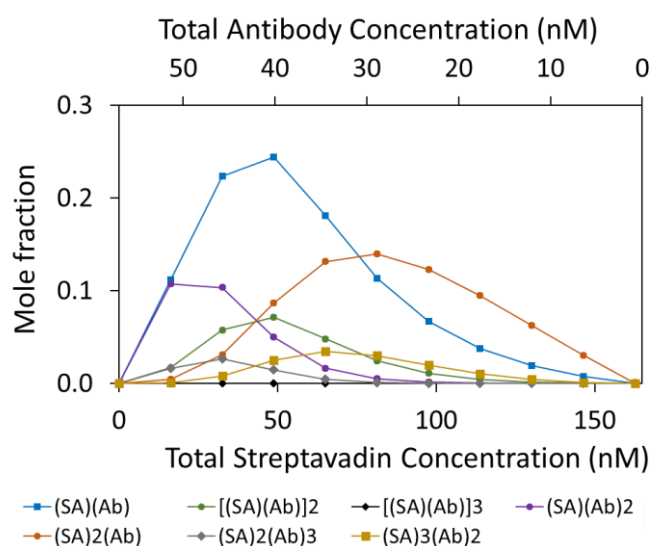
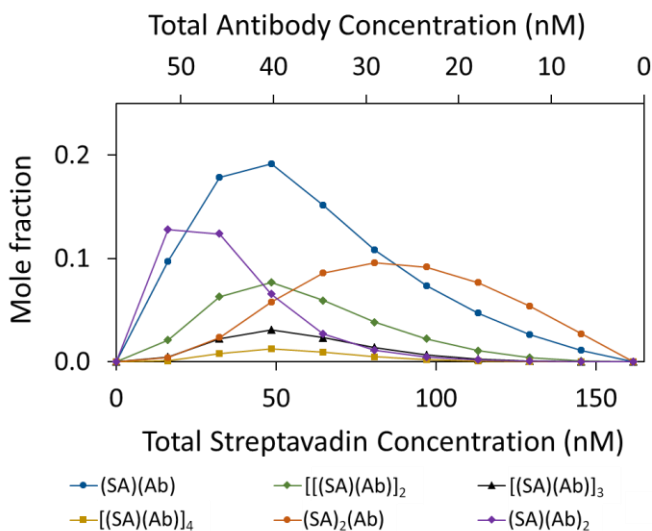
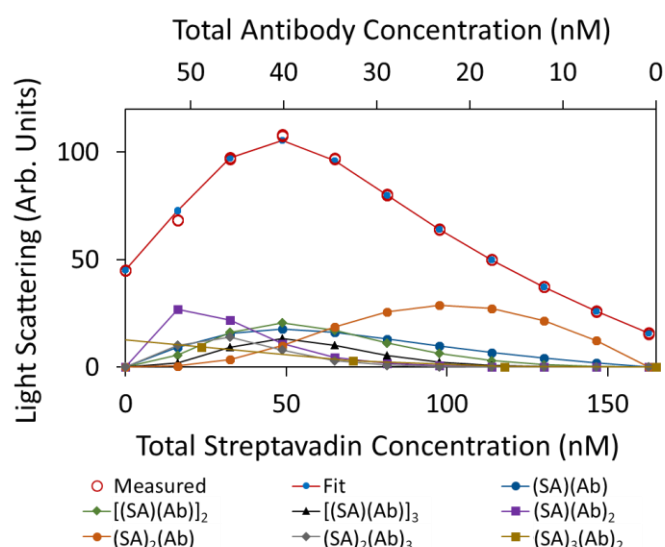
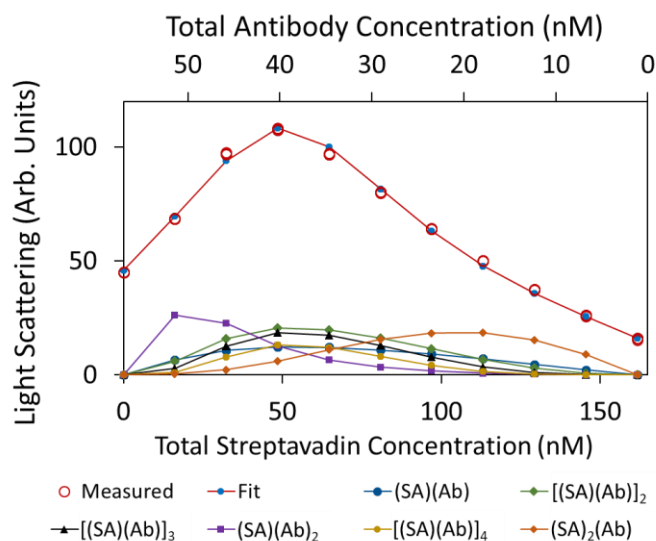


Figure 8: ISA model with the addition of 1:2 and 2:1 terms. Top: The best fit (blue circles) for the measured light scattering data (red open circles) is the sum of contributions from various terms, shown here up to 4th order. Bottom: Distribution of species across the hetero-association gradient. In both graphs, SA and Ab monomer contributions and higher-order terms are left off for clarity.

Figure 9: 2x2 association model described in the text. Top: The best fit (blue circles) for the measured light scattering data (red open circles) is made up of a combination of the indicated stoichiometries. Bottom: Distribution of species across the hetero-association gradient. In both graphs, SA and Ab monomer contributions and higher-order terms included in the fit are left off for clarity.

This model is denoted '2x2' and includes 1:1, 2:1, 1:2, 2:2, 2:3, 3:2, 3:3... terms up to $n-1:n$, $n:n$ and $n:n-1$, where n is a user-selected parameter. The best fit of this model to the SA-Ab data, shown in Figure 9, is better than previous models despite being less constrained (fewer degrees of freedom) than those used in the first and second pass: χ^2 decreased further to 0.19. This analysis yields a K_d value of 34 nM per binding site.

Conclusions

Metacomplex formation by multivalent binding partners in solution is amenable to analysis by CG-MALS to obtain absolute stoichiometries and binding affinity. In this analysis, we found that homo-tetrameric SA molecules present two binding sites for each bivalent Ab, leading to the formation of multiple stoichiometries in solution.

By measuring the absolute molecular weight of the solution, CG-MALS determined the absolute stoichiometry of

the complexes that were formed. We presented three different interpretations of the data: the infinite self-association (ISA) of (SA)(Ab) base units into [(SA)(Ab)]_n complexes; a more refined model that added 1:2 and 2:1 complexes to ISA, and a final, '2x2' model that allows for all orders of *n*-1:*n*, *n*:*n* and *n*:*n*-1 up to an arbitrary maximum *n*. The first model shows that *n*:*n* interactions account for the majority of the light scattering behavior and the molecules may be understood to present an equal number of binding sites to each other.

Under the second model, (SA)(Ab)₂ and (SA)₂(Ab) complexes contribute significantly to the total light scattering, providing strong evidence for their presence, while meeting expectations for similar single-site binding affinities across all complexes. The symmetry of each binding partner is reflected in the nearly constant affinity per binding site, *K*_d = 23 ± 7 nM, confirming that there is no cooperativity favoring the formation of higher-order complexes or appreciable inhibition to their formation under these conditions.

In the 2x2 model, the power of CG-MALS to firmly establish the complete binding scheme of this multivalent-multivalent system was revealed: though it had fewer degrees of freedom, the fit was actually better due to inclusion of all relevant complexes, confirming that both

SA and Ab present exactly two equivalent binding sites for each other.

The number of complexes, ratio of SA to Ab, and degree of self-assembly could not be predicted a priori. By this analysis, CG-MALS proves uniquely suited to investigating complex systems of macromolecules in solution.

References

1. Livnah, O., Bayer, E. A., Wilchek, M. & Sussman, J. L. Three-dimensional structures of avidin and the avidin-biotin complex. *PNAS* **90**, 5076–5080 (1993).
2. Ruigrok, V. J. B. *et al.* Kinetic and stoichiometric characterisation of streptavidin-binding aptamers. *Chembiochem* **13**, 829–836 (2012).
3. Some, D. Light-scattering-based analysis of biomolecular interactions. *Biophys Rev* **5**, 147–158 (2013).
4. Some, D. & Kenrick, S. Characterization of Protein-Protein Interactions via Static and Dynamic Light Scattering. *Protein Interactions* (2012) doi:[10.5772/37240](https://doi.org/10.5772/37240).
5. Binding Affinity and Stoichiometry of a Multivalent Protein-aptamer Association. *Wyatt Technology Corp.* <https://wyattfiles.s3-us-west-2.amazonaws.com/literature/app-notes/cg-mals/aptamer-binding.pdf> (2012).

Learn more at www.wyatt.com/CG-MALS



© Wyatt Technology Corporation. All rights reserved. No part of this publication may be reproduced, stored in a retrieval system, or transmitted, in any form by any means, electronic, mechanical, photocopying, recording, or otherwise, without the prior written permission of Wyatt Technology Corporation.

One or more of Wyatt Technology Corporation's trademarks or service marks may appear in this publication. For a list of Wyatt Technology Corporation's trademarks and service marks, please see <https://www.wyatt.com/about/trademarks>.